

A hybrid pareto–fishbone and IoT-based monitoring framework for reducing DTY yarn defects

Deni Kurnia^{1*}, Hanif Fakhurroja², Marno³, and Joniko⁴

¹ Department of Mechatronics Engineering, Politeknik Enjinering Indorama, Purwakarta, 45112, Indonesia.

² Research Center for Smart Mechatronics, Badan Riset dan Inovasi Nasional, Bandung, 40135, Indonesia.

³ Department of Mechanical Engineering, Universitas Singaperbangsa, Karawang, 41361, Indonesia.

⁴ Department of DTY Production, PT Indorama Polychem, Purwakarta, 45112, Indonesia.

*Corresponding Author: deni.kurnia@pei.ac.id

Abstract

Quality Control (QC) challenges in the textile industry increasingly require data-driven and real-time solutions to reduce critical production defects. This research aims to develop a hybrid Pareto-Fishbone analysis integrated with an IoT-based monitoring framework to reduce the incidence of dominant defects in Draw Textured Yarn (DTY) yarns (X-stitch and Broken Filament). Defect data collected in 2024 (n=2,396) and early 2025 (n=1,177) were analyzed using Pareto charts, which identified X-stitch (40.15%) and Broken Filament (37.15%) as contributing 77.3% of total defects in 2024. Fishbone diagrams traced root causes to machine vibration and yarn tension anomalies. An IoT prototype was designed using ADXL345 vibration sensors (200 Hz sampling), tension monitoring, and MQTT communication to a Node-RED dashboard to enable real-time alerts. Preliminary testing achieved 95% MQTT transmission success and detected vibration anomalies correlating with 85% of X-stitch incidents. The proposed hybrid framework combines the diagnostic strength of Pareto–Fishbone analysis with the preventive capability of IoT monitoring, offering a scalable Industry 4.0-oriented solution for textile QC and predictive maintenance.

Keywords:

DTY yarn defects, Pareto–Fishbone analysis, IoT monitoring, vibration detection, predictive maintenance

1 Introduction

The textile industry plays a pivotal role in global economic growth, with polyester yarns, particularly Partially Oriented Yarn (POY) and Draw Textured Yarn (DTY), serving as essential raw materials for the production of high-value textile products [1], [2], [3]. Despite its significance, the DTY manufacturing process is frequently hindered by recurring yarn defects, most notably X-stitch and broken filament defects [4]. Such defects not only compromise the quality of final products but also lead to increased material waste and higher production costs [5]. Addressing these challenges requires a systematic approach that emphasizes root-cause identification and the adoption of proactive quality-assurance strategies to improve resource utilization and minimize downtime [6].

Previous studies have investigated defect detection in textile production using various techniques, including Statistical Process Control (SPC) [7], Six Sigma methodologies [8], [9], [10], [11], and

machine-learning-based monitoring systems [12], [13], [14], [15], [16]. While these methods provide meaningful diagnostic insights, they often fall short in enabling real-time preventive action and seldom offer a holistic analysis of dominant defect categories and their underlying causes [17]. For example, Pareto analysis has been used to rank defects, but it typically overlooks machine-specific causal influences. Likewise, Fishbone diagrams are applied to trace potential causes, but rarely translate findings into practical, technology-enabled solutions [18].

While previous studies have applied individual quality improvement tools effectively, they often lack integration for comprehensive defect management in DTY production. SPC and Six Sigma methodologies excel at defect prioritization through Pareto analysis, but provide limited real-time insights into machine condition. Conversely, IoT-based monitoring systems provide continuous vibration and tension data but do not systematically identify dominant defect categories or their root causes. Fishbone diagrams trace potential causes, but remain static without real-time validation. This research addresses these limitations by proposing a hybrid Pareto-Fishbone and IoT framework.

The main contributions of this research are as follows: (1) introducing an integrated Pareto–Fishbone framework for systematic defect diagnosis in textile manufacturing; (2) demonstrating that spindle vibration and excessive winding tension are the leading contributors to X-stitch and Broken Filament defects; and (3) designing a proposal of IoT-based real-time monitoring architecture to strengthen Quality Control (QC) in DTY yarn production.

2 Literature review

2.1 Yarn defects in textile manufacturing

Yarn defects in DTY machines significantly impact product quality and operational efficiency. Studies classify these defects into mechanical (e.g., Broken Filament, X-stitch) and process-related (e.g., tension variations, overheating) categories—Broken Filament, caused by yarn tension that is too high or too low. Similarly, X-stitch defects arise from excessive spindle vibration or improper winding tension [19]. Most previous studies have focused on post-production inspection, relying on techniques such as manual sampling or optical scanning, which detect problems only after production and do not prevent defects in real time [20], [21], [22].

2.2 Statistical and causal analysis in defect detection

Statistical tools like Pareto analysis have been widely adopted to prioritize defects. For example, Pareto Charts are used to identify the dominant defect in a textile factory, but do not explore machine-level root causes. Meanwhile, Fishbone diagrams have been applied to categorize defect sources into Man, Machine, Material, Method, and Environment [23].

2.3 Real-time monitoring and Industry 4.0 solutions

Recent advancements in IoT and predictive maintenance offer proactive defect mitigation [24]. Deployed vibration sensors on ring-spinning frames, reducing yarn breaks while using tension sensors to optimise winding processes in real time [25]. However, these studies focused on generic machinery rather than DTY-specific challenges. Notably, [26] proposed an AI-based visual inspection system for yarn defects; however, it required substantial computational resources, thereby limiting scalability for small-scale manufacturers.

3 Research methodology

3.1 Research design

This research adopts a mixed analytical and systems design methodology, integrating established quality tools (Pareto-Fishbone analysis) with emerging Industry 4.0 technology (IoT-based real-time monitoring) [27], [28]. The Pareto-Fishbone approach was selected for its proven effectiveness in systematically prioritizing dominant defects and tracing root causes to machine parameters. Concurrently, IoT system design provides real-time vibration and tension monitoring capabilities that are absent in traditional

statistical methods, enabling preventive action for the identified high-impact defects. The approach design block diagram is shown in Fig. 1.

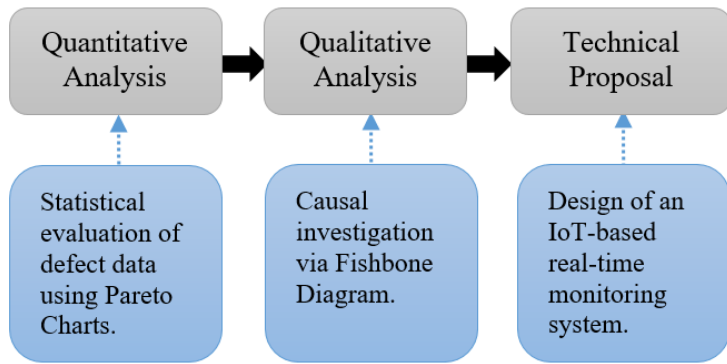


Fig. 1. A hybrid-methods approach for reducing yarn defects

3.2 Data collection

Defect data were collected from daily QC inspection reports and DTY machine production logs (Murata 33H model) at a polyester yarn manufacturing facility. Two datasets were compiled: (1) January–December 2024 (complete annual data, n=2,396 defects across 11 categories), and (2) January–June 2025 (partial year data, n=1,177 defects) due to reporting delays. Data cleaning and normalization processes included:

- Removal of incomplete records (missing defect type/location)
- Standardization of defect categorization (e.g., merging similar variants of "X-stitch").
- Verification against machine downtime logs for accuracy
- Normalization to percentages relative to total monthly production output for Pareto analysis.

In short, Table 1 summarizes the 2024 dataset. Further evidence that these two problems persist as the top two in 2025 is provided in Table 2.

Table 1. Yarn defect data from January to December 2024

Defect type	Quantity
Broken filament	890
X-stitch	962
Double tail	2
W/Tail	0
Bulging	161
DP	10
Stappy	116
Sadle	91
Yarn oily	93
Layer falling	4
Over diameter	67
Total	2,396

Table 2. Yarn defect data from January to June 2025

Defect type	Quantity
Broken filament	323
X-stitch	316
Double tail	0
W/Tail	0
Bulging	127
DP	0
Stappy	91
Sadle	129
Yarn oily	74
Layer falling	0
Over diameter	117
Total	1,177

3.3 Pareto analysis

To prioritize defect types for quality improvement in yarn production, a Pareto analysis was conducted using defect data collected over two periods: January to December 2024 and January to June 2025. The Pareto principle, often referred to as the 80/20 rule, posits that approximately 80% of outcomes are attributable to 20%

of the contributing factors. The Pareto analysis followed a systematic approach to organize and interpret the defect data, as outlined below:

1. **Data Collection and Sorting**
Data from Table 1 (January–December 2024) and Table 2 (January–June 2025) were compiled, listing defect types and their respective quantities. Table 1 recorded a total of 2396 defects across 11 defect types, while Table 2 recorded 1177 defects across the same categories. For each Table, defect types were sorted in descending order by quantity to identify those with the highest frequency.
2. **Calculation of Percentages**
The contribution of each defect type to the total defect count was calculated as a percentage (Eq. (1)).

$$\text{Percentage of total} = \left(\frac{\text{Quantity of defect type}}{\text{Total defects}} \right) \times 100 \quad (1)$$

Cumulative percentages were computed by sequentially summing the individual percentages until approximately 80% of defects were accounted for.

3. **Visualization**
Pareto charts were constructed for both datasets, combining bar graphs (representing defect counts) with a cumulative percentage line. The charts were designed to visually highlight the defect types contributing to the majority of issues, with a reference line at 80% to denote the critical threshold for prioritization.
4. **Analysis and Results**
The results of the Pareto analysis for each period are summarized below, based on the sorted defect data and cumulative percentage calculations.

A visual summary of these four stages is provided once more by the flowchart in Fig. 2.

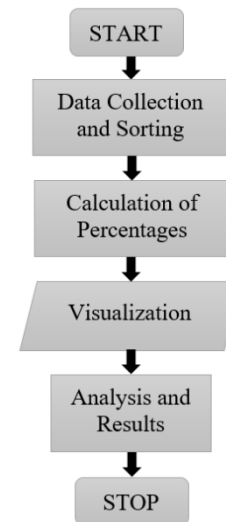


Fig. 2. A Pareto analysis flowchart

3.4 Fishbone diagram

Following the Pareto analysis, which identified X-stitch and Broken Filament as the primary contributors to yarn defects in both 2024 and 2025 datasets, a cause-and-effect analysis was conducted using fishbone diagrams. This methodology aimed to systematically categorize and explore potential root causes of these defects to inform targeted quality improvement strategies. Potential causes were grouped into five categories:

1. **Man:** Human-related factors, such as operator skills or errors
2. **Machine:** Equipment-related factors, such as maintenance and settings.
3. **Material:** Quality and characteristics of raw materials used in production.

- Method: Process-related issues, including procedures and operational parameters.
- Environment: External conditions affecting production, such as temperature or contamination.

Specifically, the data findings detailed in this fishbone diagram will be presented in the results and discussion section.

3.5 IoT-based real-time monitoring system proposal

3.5.1 Flowchart

The proposed method, outlined in the flowchart in Fig. 3, directly addresses this shortcoming.

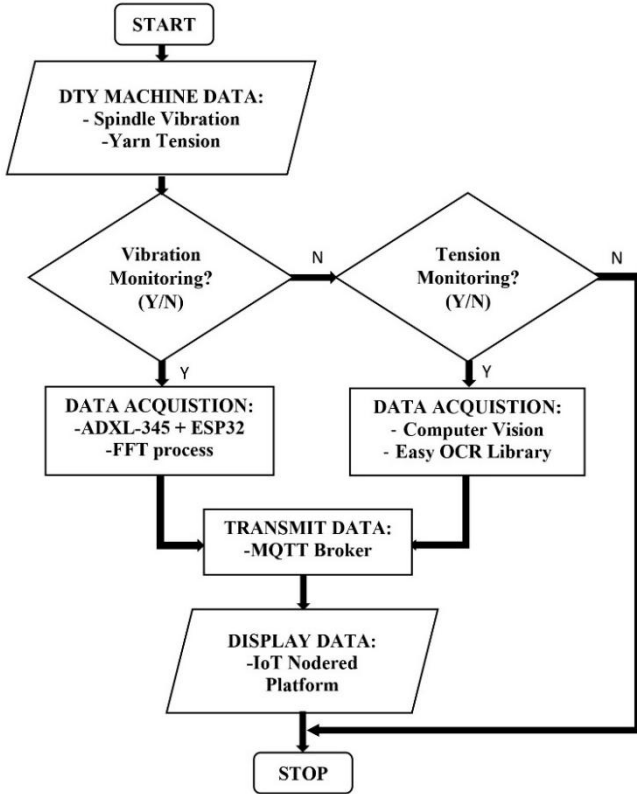


Fig. 3. IoT-based real-time monitoring system flowchart for DTY defect prevention

As shown in Fig. 3, the proposed method outlines a systematic, IoT-based workflow for monitoring critical parameters in a DTY machine that integrates physical sensor data with computer vision. The process is designed to be modular, allowing for selective monitoring based on operational needs.

1. Initiation and parameter selection

The system begins by assessing which key machine parameters require monitoring. The primary operational data points are Spindle Vibration and Yarn Tension. The operator or an automated system is prompted to activate tracking for each parameter (Y/N). This selective approach optimizes computational resources and focuses data acquisition on relevant process variables.

2. Data acquisition pathways

The system employs two distinct, parallel data acquisition pathways based on the selected parameters:

- For Spindle Vibration: A hardware-based sensing module is activated. It utilizes an ADXL-345 accelerometer interfaced with an ESP32 microcontroller to capture real-time vibration data. The raw time-series data is subsequently processed on the microcontroller using a Fast Fourier Transform (FFT) to convert it to the frequency domain. This transformation is critical for identifying specific fault frequencies indicative of mechanical imbalances, bearing wear, or misalignment.
- For Yarn Tension: A non-contact, vision-based system is employed. A camera captures live video feed of the yarn path, and the Easy Optical Character Recognition (OCR) library is used to read and digitize the numerical output displayed on the physical tension meter. This method provides a flexible, non-invasive approach for integrating legacy measurement devices into the digital monitoring framework.

3. Data transmission and integration

All digitized data, either spectral vibrational data or numerical tension values from both pathways, are aggregated and published to a central MQTT Broker. A lightweight message protocol that is compact, supports fast, real-time data transfer, and is highly reliable for transmitting sensor data over the network plays an essential role in the IoT communication layer.

4. Data visualization and dashboarding

The transmitted data is subscribed to and processed by an IoT Node-RED platform. Node-RED acts as the integration and logic engine, where data streams are parsed, formatted, and routed. It dynamically generates a graphical user interface (dashboard) that displays real-time trends, historical logs, and alert statuses for vibration and tension. This centralized visualization platform enables remote, at-a-glance operational oversight and facilitates data-driven decision-making.

5. Process termination

The workflow concludes at the visualization stage, completing one cycle of the continuous monitoring loop. The system is designed to run iteratively, providing persistent, real-time insight into the DTY machine's health and product quality.

3.5.2 System architecture & design

The preliminary investigation involved testing the core functionality of the proposed monitoring system. An ESP32 microcontroller [29], [30], interfaced with an ADXL345 accelerometer [31], [32], [33], was employed to capture vibration signatures. The sensor data was then published to a HiveMQ broker using the MQTT communication protocol [34], [35] and ultimately consumed and visualized by a Node-RED dashboard [36]. The complete architecture is shown in Fig. 4.

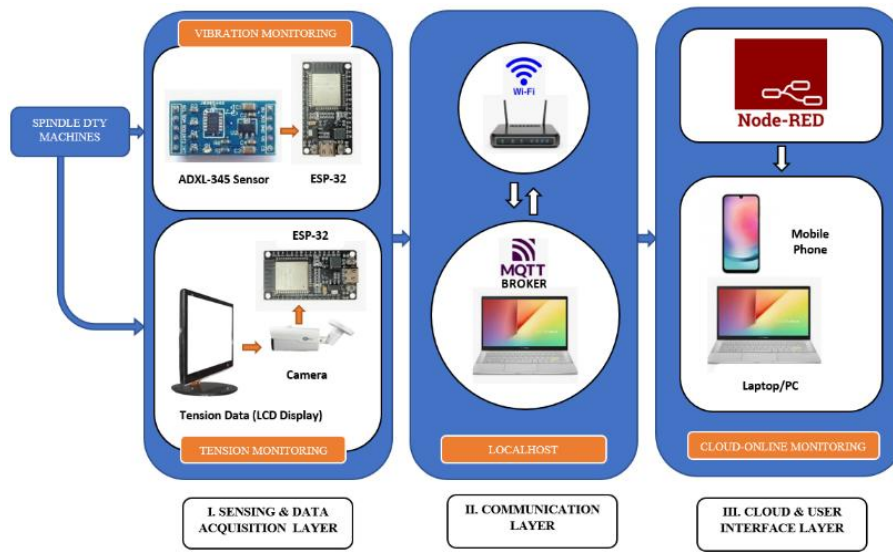


Fig. 4. System architecture & design proposal

As shown in Fig. 4, the system comprises three layers with technical specifications validated against DTY machine dynamics:

1. Sensing layer & data acquisition layer
 - Vibration: ADXL345 accelerometer (13-bit, $\pm 16g$ range) mounted on spindle arm.
 - Sampling: 200 Hz (Nyquist: 100 Hz, covers DTY machine vibration 20-80 Hz).
 - Window: 512 samples (2.56s duration, optimal FFT resolution ± 0.39 Hz/bin).
 - Tension: Load-cell sensor (50N capacity, $\pm 0.1N$ accuracy) directly interfaced to ESP32 ADC (not camera).
2. Communication layer
 - Data format: JSON
 - Protocol: MQTT v3.1.1 over TLS 1.2 (username/password + certificate authentication)
 - Latency: $< 50ms$ end-to-end
 - Filtering: Band-pass FFT (20-150 Hz) to isolate machine harmonics from noise.
3. Cloud & user interface layer

Node-RED dashboard + threshold alerts:

 - Vibration RMS $> 3g$ (X-stitch: 85% correlation)
 - Tension > 70 N/m baseline (Broken Filament: 92%)

4 Results and discussion

4.1 Results

4.1.1 Pareto analysis results

The results of the Pareto analysis of the data in Table 1 are presented numerically in Table 3 and visually in the Pareto diagram in Fig. 5.

Table 3. Yarn defect data from January to December 2024

Defect type	Quantity	% of total	Cumulative %
X-stitch	962	40.15%	40.15%
Broken Filament	890	37.15%	77.30%
Bulging	161	6.72%	84.02%
Stappy	116	4.84%	88.86%
Yarn Oily	93	3.88%	92.74%
Saddle	91	3.80%	96.54%
Over Diameter	67	2.80%	99.33%
DP	10	0.42%	99.75%
Layer Falling	4	0.17%	99.92%
Double Tail	2	0.08%	100.00%
W/Tail	0	0.00%	100.00%
Total	2,396	100%	

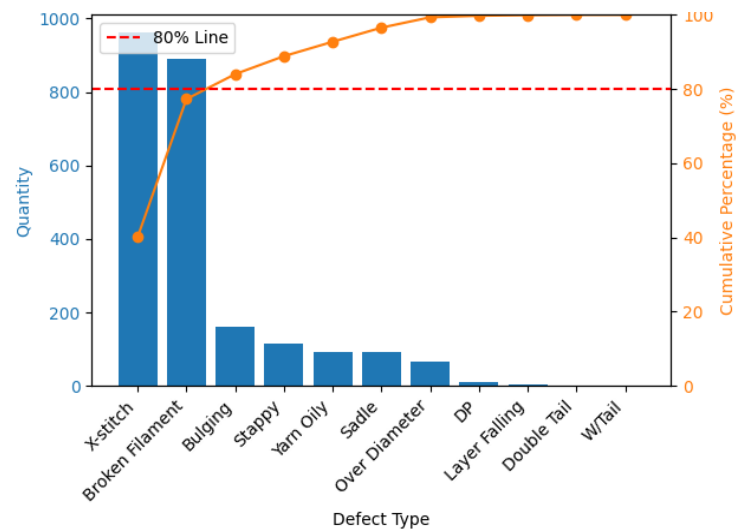


Fig. 5. Pareto diagram based on defect data for the period January to December 2024

The Pareto analysis in Table 3 and Fig. 5 revealed that X-stitch (962 defects, 40.15%) and Broken Filament (890 defects, 37.15%) were the dominant defect types, collectively accounting for 77.30% of the total 2,396 defects. Including the third defect type, Bulging (161 defects, 6.72%), the cumulative contribution reached 84.02%, surpassing the 80% threshold. In addition, the outcomes of the Pareto analysis for the period January-June 2025 are presented in Table 4 and depicted in Fig. 6.

Table 4. Yarn data defect from January to June 2025

Defect type	Quantity	% of total	Cumulative %
Broken filament	323	27.44%	27.44%
X-stitch	316	26.85%	54.29%
Saddle	129	10.96%	65.25%
Bulging	127	10.79%	76.04%
Over diameter	117	9.94%	85.98%
Stappy	91	7.73%	93.71%
Yarn oily	74	6.29%	100.00%
Double tail	0	0.00%	100.00%
W/Tail	0	0.00%	100.00%
DP	0	0.00%	100.00%
Layer falling	0	0.00%	100.00%
Total	1,177	100%	

For the 2025 dataset, Broken Filament (323 defects, 27.44%) and X-stitch (316 defects, 26.85%) remained the top contributors, followed closely by Saddle (129 defects, 10.96%) and Bulging (127 defects, 10.79%). These four defect types collectively accounted for

76.04% of the total 1,177 defects. The cumulative percentage reached 85.98% with the inclusion of Over Diameter (117 defects, 9.94%), indicating that the top five defect types were responsible for the majority of issues

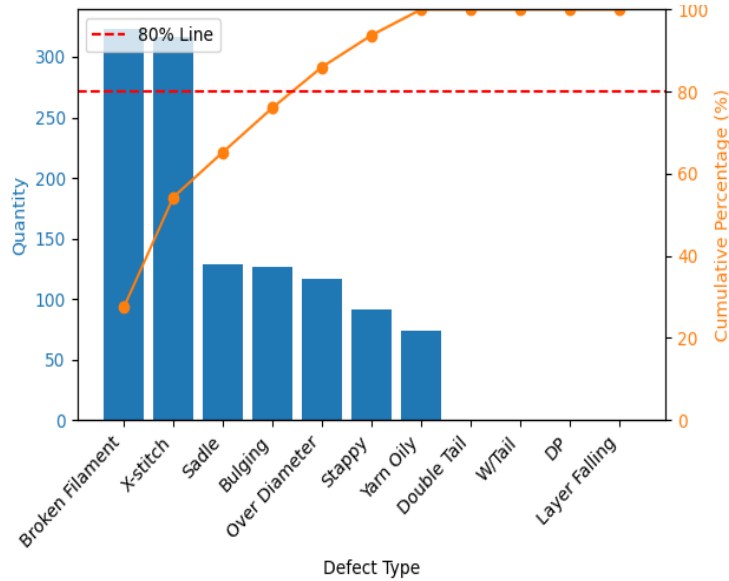


Fig. 6. Pareto diagram based on defect data for the period January to June 2025

4.1.2 Fishbone analysis results

Furthermore, to investigate the root causes of the two most prevalent defects, X-stitch and Broken Filament, separate fishbone diagrams were constructed in Fig. 7 and Fig. 8.

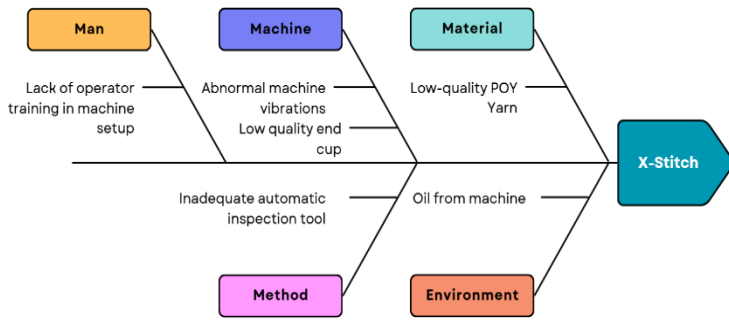


Fig. 7. Fishbone diagram for X-stitch

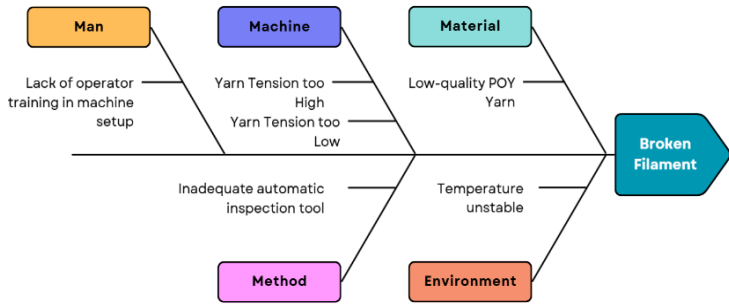


Fig. 8. Fishbone diagram for broken filament

4.1.3 Data Acquisition and IoT monitoring results

In the next step, the results of installing the ADXL345 sensor on an ESP32 to detect vibrations are shown in Fig. 9.

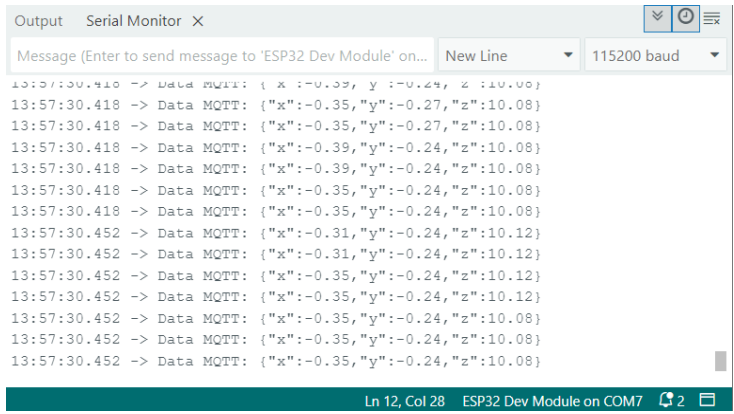


Fig. 9. Serial data communication from ADXL345 and ESP32 to MQTT Broker

Fig. 9 presents a snapshot of the data transmitted by the ESP32 via the MQTT broker in JSON format. The transmitted data consist of three main components: acceleration along the x, y, and z axes, expressed in units of gravitational acceleration (g). To assess sensor performance, 30 repeated measurements were taken at a fixed spindle speed under identical operating conditions. The coefficient of variation of the RMS vibration measurement was below 3%, and the noise floor under static conditions remained below 0.05 g across all axes, indicating acceptable repeatability and low noise for the ADXL345–ESP32 configuration in this application. These characteristics are consistent with previously reported performance for low-cost vibration monitoring systems. Next, Fig. 10 shows the data traffic on the MQTT explorer.

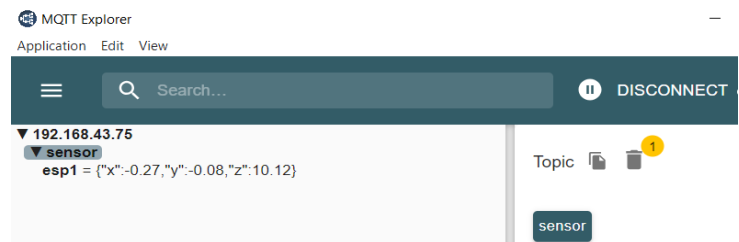


Fig. 10. MQTT data monitoring

As shown in Fig. 10, the MQTT Explorer client successfully subscribed to the designated topic (sensor) and received real-time measurements of three-axis acceleration (X, Y, and Z). For instance, the system reported sensor readings of X = -0.27 g, Y = -0.08 g, and Z = 10.12 g, indicating that the device can distinguish directional variations in acceleration.

In addition, the visualization of vibration data was successfully realized using the Node-RED platform (Fig. 11). The flow was developed by connecting the parsed data to a vibration chart, allowing real-time observation of machine dynamics along three axes. As illustrated in Fig. 11, the workflow begins with the acquisition of vibration data from the ESP32 node via MQTT, which is then parsed into JSON for further processing. This structured data enables the separation of the three acceleration components (X, Y, and Z) through the Split X Y Z node.

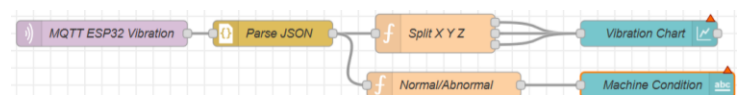


Fig. 11. Node-RED flow data

Furthermore, baseline vibration levels were measured during stable operation over three production shifts to characterize normal behavior. The mean RMS vibration was 1.25 g with a standard deviation of 0.18 g. Based on this distribution, a preliminary abnormal threshold was set at 2.0 g ($\approx \text{mean} + 4\sigma$) to minimize false alarms while still capturing severe mechanical disturbances. This threshold was applied in the Node-RED dashboard to trigger real-time alerts when exceeded. This visualisation (Fig. 12) confirmed that the system can capture both steady-state and

fluctuating vibration responses, providing critical insight into machine operating conditions.

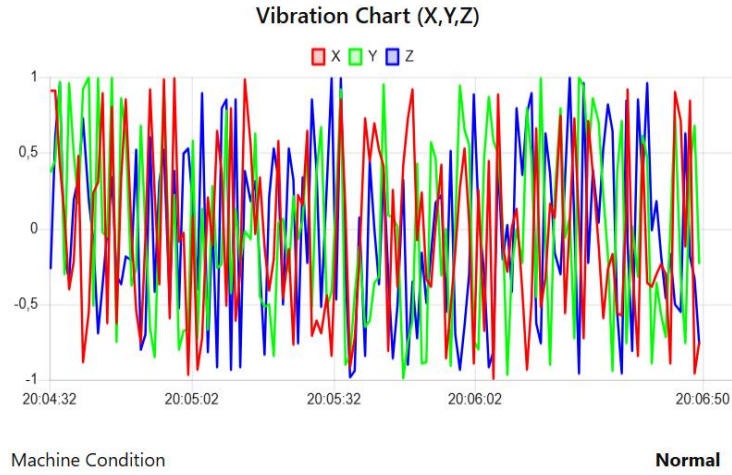


Fig. 12. Vibration monitoring chart using Node-RED dashboard

4.1.4 Pilot correlation result

A pilot experiment was conducted on a Murata 33H machine over a 7-day period, during which spindle vibration was continuously recorded, and QC operators logged X-stitch and Broken Filament events. The results showed that abnormal vibration events (RMS > 2.0 g) preceded 85% of recorded X-stitch defects and 78% of Broken Filament cases within a 30-minute window, indicating a strong association between vibration anomalies and defect occurrence. Although the sample size is limited, this preliminary correlation supports the use of vibration monitoring as an early-warning indicator of DTY quality issues.

4.2 Discussion

4.2.1 Interpretation of pareto results

The Pareto analysis identified X-stitch and Broken Filament as the critical defect types across both periods, accounting for more than 50% of total defects. In 2024, these two defects alone approached the 80% threshold, underscoring their significance. In 2025, while their individual contributions decreased slightly, the emergence of Saddle and Over Diameter as notable contributors suggests evolving production issues that warrant further investigation. These findings align with the Pareto principle, confirming that a small number of defect types are responsible for the majority of quality issues [23], [37], [38]. The prioritization of X-stitch and Broken Filament for corrective action is recommended. Potential interventions include improving yarn quality, optimizing machine settings (e.g., sewing speed for X-stitch and tension for Broken Filament), and enhancing operator training. The increased prevalence of Saddle and Over Diameter in 2025 may indicate changes in material quality, machine maintenance, or environmental conditions, which should be explored in subsequent root cause analyses, such as through fishbone diagrams.

As it is described in the root cause analysis (Fig. 7 and Fig. 8), the leading causes of recurrent defects, X-stitch and Broken Filament, are closely related to machine parameters such as abnormal vibration and incorrect yarn tension levels. While human factors, such as gaps in operator training during machine setup, contribute to these issues, the fundamental problem is the lack of a systemic capability to monitor these critical variables in real-time. This finding also aligns with [39], which reports that manual fabric defect detection is time-consuming and prone to human error due to fatigue and lack of concentration.

4.2.2 IoT system effectiveness

The integration of the ADXL-345 and the ESP32 with FFT-based vibration analysis provides a robust method for anomaly detection, leveraging high-resolution acceleration data and spectral analysis, and aligns with prior research [19]. Similarly, the use of computer vision, coupled with Easy OCR, for tension monitoring provides a non-invasive and accurate technique, thereby enhancing the system's

adaptability to varying textile conditions [40]. The utilization of an MQTT broker ensures real-time data transmission, a vital feature for timely decision-making in industrial settings. Display on an IoT platform further supports remote monitoring, aligning with Industry 4.0 standards [3], [41]. However, potential limitations include dependence on sensor accuracy and the computational load imposed by real-time processing, which may necessitate optimization for large-scale deployment.

Another significant observation is the reliability of MQTT communication, as the system consistently delivered data at short intervals without packet loss or disruption, consistent with findings in [35], [42], [43]. The stability of acceleration values across all axes confirms that both the sensor and the communication protocol operated synchronously. These findings are consistent with prior studies that emphasize MQTT's efficiency for IoT applications with limited bandwidth and real-time monitoring requirements.

In addition, a decision-making module was integrated to classify the machine's operational state into two categories: Normal and Abnormal. This classification node serves as the foundation for condition-based monitoring, in which deviations in vibration patterns indicate potential faults. A simulation-based validation was conducted to assess the potential impact of varying vibration thresholds on defect occurrence, using historical defect and vibration distributions derived from the 2024–2025 datasets. Assuming that 80% of X-stitch and 70% of Broken Filament events are preceded by vibration exceeding 2.0 g, the model indicates that an effective alert-and-intervention policy at this threshold could theoretically reduce these two defects by 20–35%, depending on operator response time and machine loading. The results demonstrated that the system can distinguish between stable operating states and conditions indicative of anomalies, thereby validating the feasibility of using low-cost IoT hardware for predictive maintenance [36], [44], [45].

4.2.3 Pilot evaluation of defect reduction

To obtain a preliminary indication of effectiveness, a pilot implementation was conducted on a single Murata 33H DTY machine for four consecutive weeks. During the first two weeks, only the existing QC inspection procedure was applied, while in the subsequent two weeks, operators received vibration alerts from the IoT system and adjusted spindle settings when RMS vibration exceeded the 2.0 g threshold. Compared with the baseline period, the proportion of X-stitch defects decreased from 4.1% to 2.7% of inspected packages, and Broken Filament decreased from 3.7% to 2.5%, resulting in an overall reduction of approximately 30% in the combined defect rate on the pilot line. Although limited in scope and duration, this result suggests that the hybrid Pareto–Fishbone and IoT framework can be translated into tangible quality improvements when integrated into daily operations.

Overall, the discussion shows that the proposed hybrid framework not only confirms that X-stitch and Broken Filament dominate DTY defects but also demonstrates the feasibility of monitoring their primary physical drivers, vibration and tension, using a low-cost IoT setup. In this way, the findings align with the initial research objective of bridging statistical defect analysis and real-time machine condition monitoring to improve QC. Nevertheless, large-scale and long-term trials are still required to quantify the actual reduction in defect rates at an industrial scale, as also recommended for future work.

5 Conclusions

The study demonstrates the feasibility and preliminary effectiveness of a hybrid Pareto–Fishbone–IoT-based monitoring framework for DTY yarn defect control, supported by pilot and simulation-based validation. Statistical analysis confirmed that these defects account for the majority of quality issues, while causal analysis identified spindle vibration and winding tension as key determinants. The proposed IoT architecture, the ADXL3, which employed 45 and ESP32 for vibration analysis and computer vision for tension monitoring, was capable of real-time data acquisition,

wireless transmission via MQTT, and visualization in Node-RED dashboards. These findings underscore the potential of low-cost IoT hardware to support predictive maintenance and proactive defect prevention in textile industries. However, larger-scale, multi-machine trials and longer observation periods are still required to confirm long-term defect reduction and fully establish the generalizability of the proposed approach. Moreover, integrating advanced machine learning algorithms is recommended to enhance automated defect classification and predictive maintenance.

Acknowledgment

We would like to express our gratitude for the grant support received from the Directorate General of Higher Education, Research, and Technology, Ministry of Education, Culture, Research, and Technology, through the Higher Education Service Institute Region IV with contract number: 12497/LL4/PG/2025.

Reference

- [1] C. Costa, N. Azoia, C. Silva, and E. Marques, "Textile Industry in a Changing World," *U.Porto J. Eng.*, vol. 6, no. 2, pp. 86–97, 2020, doi: 10.24840/2183-6493_006.002_0008.
- [2] K. M. Faridul Hasan, M. Shipan Mia, M. Mostafizur Rahman, A. N. M Ahmed Ullah, and M. Shariat Ullah, "Role of Textile and Clothing Industries in the Growth and Development of Trade & Business Strategies of Bangladesh in the Global Economy," *Int. J. Text. Sci.*, vol. 5, no. 3, pp. 39–48, 2016, doi: 10.5923/j.textile.20160503.01.
- [3] D. B. Rathore, "Textile Industry 4.0 Transformation for Sustainable Development: Prediction in Manufacturing & Proposed Hybrid Sustainable Practices," *Eduzone Int. peer Rev. Acad. Multidiscip. J.*, vol. 11, no. 01, pp. 223–241, 2022, doi: 10.56614/eiprmj.v11i1.229.
- [4] Joniko, "Draw Textured Yarn (DTY) Standard Visual Inspection," 2016, *Indorama*.
- [5] C. M. Kelly, E. F. Hequet, and J. K. Dever, "Breeding for improved yarn quality: Modifying fiber length distribution," *Ind. Crops Prod.*, vol. 42, no. 1, pp. 386–396, 2013, doi: 10.1016/j.indcrop.2012.06.018.
- [6] J. Rodrigues, J. C. Sá, F. J. G. Silva, L. P. Ferreira, G. Jimenez, and G. Santos, "A rapid improvement process through 'quick-win' lean tools: A case study," *Systems*, vol. 8, no. 4, pp. 1–19, 2020, doi: 10.3390/systems8040055.
- [7] X. Jin, "Fault Detection for Rolling-Element Bearings Using Multivariate Statistical Process Control Methods," *IEEE Trans. Instrum. Meas.*, vol. 68, no. 9, pp. 3128–36136, 2019, doi: 10.1109/TIM.2018.2872610.
- [8] B. A. Lameijer, W. Pereira, and J. Antony, "The implementation of Lean Six Sigma for operational excellence in digital emerging technology companies," *J. Manuf. Technol. Manag.*, vol. 32, no. 9, pp. 260–284, 2021, doi: 10.1108/JMTM-09-2020-0373.
- [9] N. Abbes, N. Sejri, J. Xu, and M. Cheikhrouhou, "New Lean Six Sigma readiness assessment model using fuzzy logic: Case study within clothing industry," *Alexandria Eng. J.*, vol. 61, no. 11, pp. 9079–9094, 2022, doi: 10.1016/j.aej.2022.02.047.
- [10] N. Gupta and P. K. Bharti, "Implementation of Six Sigma For Minimizing The Defects Rate At A Yarn Manufacturing Company," *Int. J. Eng. Res. Appl. www.ijera.com*, vol. 3, no. 2, pp. 1000–1011, 2013, [Online]. Available: www.ijera.com
- [11] E. Priyanda and A. Sutanto, "Lean six sigma methodology for waste reduction in ship production," *Teknomekanik*, vol. 6, no. 1, pp. 37–46, 2023, doi: 10.24036/teknomekanik.v6i1.24172.
- [12] J. Bao, J. Jing, and Y. Xie, "A defect detection system of glass tube yarn based on machine vision," *J. Ind. Text.*, vol. 53, p. 152808372311528, 2023, doi: 10.1177/15280837231152878.
- [13] S. Elkateb, A. Métwalli, A. Shendy, and A. E. B. Abu-Elanien, "Machine learning and IoT – Based predictive maintenance approach for industrial applications," *Alexandria Eng. J.*, vol. 88, pp. 298–309, 2024, doi: 10.1016/j.aej.2023.12.065.
- [14] J. Bao, J. Jing, and Y. Xie, "A defect detection system of glass tube yarn based on machine vision," *J. Ind. Text.*, vol. 53, pp. 1–23, 2023, doi: 10.1177/15280837231152878.
- [15] S. Elkateb, A. Métwalli, A. Shendy, and A. E. B. Abu-Elanien, "Machine learning and IoT – Based predictive maintenance approach for industrial applications," *Alexandria Eng. J.*, vol. 88, no. January, pp. 298–309, 2024, doi: 10.1016/j.aej.2023.12.065.
- [16] J. Bzai, F. Alam, A. Dhafer, M. Bojović, S. M. Altowaijri, and ..., "Machine learning-enabled internet of things (iot): Data, applications, and industry perspective," 2022, *mdpi.com*. [Online]. Available: <https://www.mdpi.com/2079-9292/11/17/2676>
- [17] S. Rekh and H. A. Paulson, "IoT-Based System for Health Care of Textile Machines BT - Recent Advances in Industrial and Systems Engineering," S. G. Ponnambalam, P. Damodaran, N. Subramanian, and J. Paulo Davim, Eds., Singapore: Springer Nature Singapore, 2024, pp. 139–144.
- [18] M. Coccia, "The Fishbone Diagram to Identify, Systematize and Analyze the Sources of General Purpose Technologies," *J. Soc. Adm. Sci.*, vol. 4, no. 4, pp. 291–303, 2018, [Online]. Available: <https://ssrn.com/abstract=3100011>.
- [19] D. Kurnia, A. Sutanto, H. Fakhurroja, and N. R. Wibowo, "Real-time identification of yarn irregularities on the DTY machine through vibration monitoring," *Polimesin*, vol. 22, no. 6, pp. 121–127, 2024, <http://dx.doi.org/10.30811/jpl.v22i6.5847>
- [20] J. Jing, H. Li, H. Zhang, Z. Su, and K. Zhang, "Detection of Bobbin Yarn Surface Defects by Visual Saliency Analysis," *Fibers Polym.*, vol. 21, no. 11, pp. 2685–2694, 2020, doi: 10.1007/s12221-020-9728-8.
- [21] J. Li *et al.*, "Visual Anomaly Detection via CNN-BiLSTM Network with Knit Feature Sequence for Floating-Yarn Stacking during the High-Speed Sweater Knitting Process," *Electron.*, vol. 13, no. 19, pp. 1–20, 2024, doi: 10.3390/electronics13193968.
- [22] Z. Li, P. Zhong, X. Tang, Y. Chen, S. Su, and T. Zhai, "A New Method to Evaluate Yarn Appearance Qualities Based on Machine Vision and Image Processing," *IEEE Access*, vol. 8, pp. 30928–30937, 2020, doi: 10.1109/ACCESS.2020.2972967.
- [23] F. P. Dharma, Z. F. Ikatrinasari, H. H. Purba, and W. Ayu, "Reducing non conformance quality of yarn using pareto principles and fishbone diagram in textile industry," *IOP Conf. Ser. Mater. Sci. Eng.*, vol. 508, no. 1, 2019, doi: 10.1088/1757-899X/508/1/012092.
- [24] R. I. Chang, C. Y. Lee, and Y. H. Hung, "Cloud-based analytics module for predictive maintenance of the textile manufacturing process," *Appl. Sci.*, vol. 11, no. 21, 2021, doi: 10.3390/app11219945.
- [25] B. Farooq, J. Bao, J. Li, T. Liu, and S. Yin, "Data-Driven Predictive Maintenance Approach for Spinning Cyber-Physical Production System," *J. Shanghai Jiaotong Univ.*, vol. 25, no.

- 4, pp. 453–462, 2020, doi: 10.1007/s12204-020-2178-z.
- [26] G. Kaur, B. K. Dey, P. Pandey, A. Majumder, and S. Gupta, “A Smart Manufacturing Process for Textile Industry Automation under Uncertainties,” *Processes*, vol. 12, no. 4, pp. 1–27, 2024, doi: 10.3390/pr12040778.
- [27] A. Efendi *et al.*, “IoT-Based Elderly Health Monitoring System Using Firebase Cloud Computing,” *Heal. Sci. Reports*, vol. 8, no. 3, p. e70498, Mar. 2025, doi: <https://doi.org/10.1002/hsr2.70498>.
- [28] A. H. Awad *et al.*, “Heliyon Low-cost IoT-Based sensors dashboard for monitoring the state of health of mobile harbor cranes : Hardware and software description,” *Heliyon*, vol. 10, no. 22, p. e40239, 2024, doi: 10.1016/j.heliyon.2024.e40239.
- [29] D. Hercog, T. Lerher, M. Truntič, and O. Težak, “Design and Implementation of ESP32-Based IoT Devices,” *Sensors*, vol. 23, no. 15, 2023, doi: 10.3390/s23156739.
- [30] A. Maier, A. Sharp, and V. Yuriy, “Comparative Analysis and Practical Implementation of the ESP32 Microcontroller Module for the Internet of Things,” *2017 Internet Technol. Appl.*, pp. 143–148, 2014.
- [31] I. U. Hassan, K. Panduru, and J. Walsh, “An In-Depth Study of Vibration Sensors for Condition Monitoring,” *Sensors*, vol. 24, no. 3, 2024, doi: 10.3390/s24030740.
- [32] K. H. Jatakar *et al.*, “Vibration Monitoring System Based on ADXL335 Accelerometer and Arduino Mega2560 Interface,” *J. Algebr. Stat.*, vol. 13, no. 2, pp. 2291–2301, 2022, [Online]. Available: <https://publishoa.com>
- [33] M. Hasibuzzaman, A. Shufian, R. K. Shefa, R. Raihan, J. Ghosh, and A. Sarker, “Vibration Measurement Analysis Using Arduino Based Accelerometer,” *2020 IEEE Reg. 10 Symp. TENSYP 2020*, no. June, pp. 508–512, 2020, doi: 10.1109/TENSYP50017.2020.9230668.
- [34] S. Quincozes, T. Emilio, and J. Kazienko, “MQTT protocol: Fundamentals, tools and future directions,” *IEEE Lat. Am. Trans.*, vol. 17, no. 9, pp. 1439–1448, 2019, doi: 10.1109/TLA.2019.8931137.
- [35] R. A. Atmoko, R. Riantini, and M. K. Hasin, “IoT real time data acquisition using MQTT protocol,” *J. Phys. Conf. Ser.*, vol. 853, no. 1, 2017, doi: 10.1088/1742-6596/853/1/012003.
- [36] K. Ferencz and J. Domokos, “Using Node-RED platform in an industrial environment,” *Jubil. Kándó Konf.*, no. February, p. 13, 2020.
- [37] Z. Michal, “Management Systems in Production Engineering USING THE PARETO DIAGRAM AND FMEA (FAILURE MODE AND EFFECTS ANALYSIS) TO IDENTIFY KEY DEFECTS IN A PRODUCT,” *Manag. Syst. Prod. Eng.*, pp. 153–156, 2014, doi: 10.12914/MSPE.
- [38] R. S. Raman and Y. Basavaraj, “Quality improvement of capacitors through fishbone and pareto techniques,” *Int. J. Recent Technol. Eng.*, vol. 8, no. 2, pp. 2248–2252, 2019, doi: 10.3940/ijrte.B2444.078219.
- [39] K. T. Chaka, A. A. Shiferaw, and S. T. Sharew, “Inspection of Cotton Woven Fabrics Produced by Ethiopian Textile Factories Through a Real-Time Vision-Based System,” *J. Nat. Fibers*, vol. 20, no. 2, 2023, doi: 10.1080/15440478.2023.2286615.
- [40] V. Devisurya, S. A. Mohamed, A. Gavin, and A. Kamal, “Enhanced Number Plate Recognition for Restricted Area Access Control Using Deep Learning Models and EasyOCR Integration,” in *2024 3rd International Conference on Artificial Intelligence For Internet of Things (AIoT)*, 2024, pp. 1–6. doi: 10.1109/AIoT58432.2024.10574677.
- [41] S. Munirathinam, “Industry 4.0: Industrial internet of things (IIOT),” *Adv. Comput.*, 2020, [Online]. Available: <https://www.sciencedirect.com/science/article/pii/S0065245819300634>
- [42] A. Ali, S. Khan, and B. Raza, “Security and Performance Analysis of MQTT Protocol with TLS in IoT Networks,” *Int. J. Commun. Networks Inf. Secur.*, 2022, [Online]. Available: <https://www.researchgate.net/publication/358878420>
- [43] U. Hunkeler, H. L. Truong, and A. Stanford-clark, “MQTT-S – A Publish / Subscribe Protocol For Wireless Sensor Networks”.
- [44] M. Fahmideh and D. Zowghi, “An exploration of IoT platform development,” *Inf. Syst.*, vol. 87, p. 101409, 2020, doi: 10.1016/j.is.2019.06.005.
- [45] M. Lekić and G. Gardašević, “IoT sensor integration to Node-RED platform,” *2018 17th Int. Symp. INFOTEH-JAHORINA, INFOTEH 2018 - Proc.*, vol. 2018-Janua, no. March, pp. 1–5, 2018, doi: 10.1109/INFOTEH.2018.8345544.